ELSEVIER

Journal of Nuclear Materials 313–316 (2003) 274–278

journal of nuclear materials

www.elsevier.com/locate/jnucmat

Re-emission of hydrogen implanted into graphite by helium ion bombardment

B. Tsuchiya [a,*], K. Morita [b], S. Yamamoto [c], S. Nagata [a], N. Ohtsu [a], T. Shikama [a], H. Naramoto [d]

[a] *Institute for Materials Research, Tohoku University, 2-1-1, Katahira, Aoba-ku, Sendai 980-8577, Japan*
[b] *Department of Crystalline Materials Science, Graduate School of Engineering, Nagoya University, Furo-cho, Chikusa-ku, Nagoya 464-8603, Japan*
[c] *Department of Materials Development, Japan Atomic Energy Research Institute, Watanuki-cho, Takasaki 370-1292, Japan*
[d] *Advanced Science Research Center, Japan Atomic Energy Research Institute, Watanuki-cho, Takasaki 370-1292, Japan*

Abstract

Helium ion-induced re-emission of hydrogen implanted in graphite with 5 keV H_2^+ ion beam at room temperature has been investigated in the energy range from 60 to 200 keV, by means of a high energy elastic recoil detection method with 16 MeV O^{5+} ion beam. The hydrogen concentrations in graphite rapidly decrease with increasing the He^+ ion fluence and reach a constant value of $H/C \cong 0.2$. The re-emission rates of hydrogen from graphite increase with decreasing incident energy of the He^+ ion. The He^+ ion-induced detrapping cross-sections have been evaluated by analyzing the experimental data with mass balance equations including elementary processes such as detrapping, trapping and local molecular re-combination between an activated hydrogen atom and a trapped one. The elastic displacement collisions with energetic carbon recoils produced by He^+ ion bombardments are dominant for the detrapping of hydrogen in the range of the incident energies.

PACS: 06.30.B; 39.10; 41.75.A
Keywords: Ion-induced re-emission; Hydrogen; Helium ion bombardment; De-trapping cross-section; Mass balance equation

1. Introduction

In magnetically confined fusion devices, it has been demonstrated that low-Z materials (e.g. graphite) used as plasma facing components well operate wall pumping for large fluences of hydrogen isotopes in the beginning of a discharge. In order to achieve the ignition condition during long term D–T discharges, it is important to predict the transient re-cycling fluxes of each hydrogen species from the plasma facing components and to control the D/T ratio in the fueling. Previously, for our group the re-emissions of H and D implants in graphite by D^+ and H^+ ion bombardments with energies of keV have been studied using an elastic recoil detection (ERD) technique with 1.7 MeV He^+ ion beam. The ion-induced detrapping cross-sections of H and D by D^+ and H^+ ion impacts, respectively, have been determined by fitting solutions of mass balance equations which include the elementary processes: ion-induced detrapping, trapping and local molecular re-combination between an activated hydrogen atom and a trapped one to the experimental data [1,2]. Moreover, the re-emissions of H and D implanted into graphite by 0.8–1.9 MeV He^+ ion bombardments have been also investigated and the ion-induced detrapping cross-sections have been determined using the mass balance equations. The energy dependence and the isotope effect of the

* Corresponding author. Tel.: +81-22 215 2063; fax: +81-22 215 2061.
E-mail address: tsuchiya@imr.tohoku.ac.jp (B. Tsuchiya).

0022-3115/03/$ - see front matter
PII: S0022-3115(02)01341-7

ion-induced detrapping cross-sections have been described by the theoretical one, which are assumed as the average of the cross-sections for elastic displacements of trapped hydrogen isotope by energetic carbon recoils in cascade collisions initiated by MeV He^+ ions [3–5].

In this paper, the experimental data on the re-emissions of H implants by He^+ ion bombardments in the energy range of 60–200 keV are reported. The He^+ ion-induced detrapping cross-sections are analyzed using the mass balance equations and are shown as a function of the energy.

2. Experiments

Specimens used in the present study were isotropic graphite (IG110U) plates with the dimension of $10 \times 15 \times 1$ mm^3. The surface was mechanically polished with a diamond paste. The specimen was placed on a manipulator in contact with a ceramic heater in a vacuum chamber evacuated to pressure of 1.3×10^{-5} Pa and heated at a temperature of 1273 K to remove small amounts of residual hydrogen. The temperature of the specimen was measured with an alumel–chromel thermocouple in contact with the surface. Implantation of hydrogen into the specimens was made up to saturation with 5 keV H_2^+ ion beam at room temperature. The projected range was 35 nm [6] and the saturation concentration as measured to be close to $H/C = 0.4$ was consistent with that reported in Ref. [7].

The re-emission experiments were performed using a dual ion beam analysis system with a 3 MV tandem accelerator and a 400 kV implanter, developed at the TIARA facility in JAERI/Takasaki. The specimens were irradiated at room temperature with 60, 100 and 200 keV He^+ ions, which were generated from the implanter. The incident angle was 50° to the surface normal of the specimens. The incident energies were selected for He^+ ions to exceed the implantation depth of hydrogen retained in graphite completely. At several He^+ ion fluences, the concentration of hydrogen retained in the specimen was measured by means of the high energy elastic recoil detection (H-ERD) method with 16 MeV $^{16}O^{5+}$ ion beam from the tandem accelerator. For the H-ERD measurement, the O^{5+} ions were incident at the angle of 75° to the surface normal of the specimens and both the hydrogen and helium recoiled were detected at the scattering angle of 30° to the incident ion direction. An Al absorber foil of 12 μm thickness was installed in front of the detector. Simultaneously, Rutherford backscattering spectrometry (RBS) measurements were carried out at the backscattering angle of 90° to the incident ion direction as an ion fluence monitor. Since the O^{5+} ion fluence was so low (about 10^{12} ions/cm^2 s $\times 10^3$ s) to take one energy spectrum by ERD, the temperature rise was not detected by the thermocouple measurement and the hydrogen release was not also found during the ERD measurements.

3. Experimental results and discussion

3.1. Re-emission of H due to He^+ ion bombardment

Fig. 1 shows typical H-ERD spectra which are obtained after implantation with 5 keV H_2^+ ions to saturation and 100 keV He^+ ion bombardment at the ion fluence of 4.8×10^{16} ions/cm^2 at room temperature. The absolute value of the O^{5+} ion fluence monitored by RBS was calibrated using those estimated from the product of the current and the irradiation time for several H-ERD measurements. The vertical and horizontal axes represent the concentrations of H and He retained in graphite and the energies of H and He recoiled by elastic collisions with 16 MeV O^{5+} ions, respectively. It is seen from Fig. 1 that the concentration of H decreases and that of He increases, after He^+ ion irradiation. The number of hydrogen retained in graphite are plotted in Fig. 2 as a function of the He^+ ion fluence for the incident energies of 60, 100 and 200 keV, where the content of retained H is normalized to the initial one, namely to the saturation value. There exist two stages in the re-emission of hydrogen from graphite as the ion fluence increases. The initial stage is characterized by fast re-emission, which can be explained by about zero concentration of vacant trapping sites in graphite in conditions of saturation. Respectively re-trapping of detrapped hydrogen is impossible. The second stage is characterized by slow decrease, and this is possibly due to strong re-trapping of the detrapped hydrogen atom into vacant trapping sites

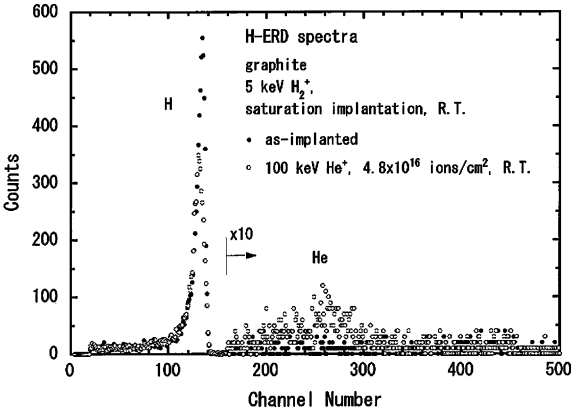

Fig. 1. Typical H-ERD spectra of H and He recoiled from graphite with 16 MeV O^{5+} ion beam. (•) and (◦) represent H-ERD spectra measured after the saturation implantation with 5 keV H_2^+ ions at room temperature and after the 100 keV He^+ ion bombardment at the fluence of 4.8×10^{16} ions/cm^2 and room temperature, respectively.

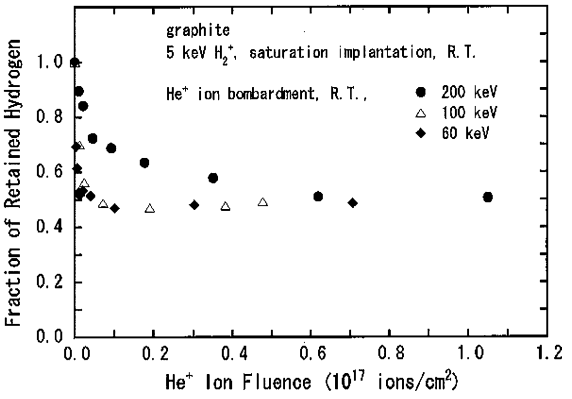

Fig. 2. Fractions of retained hydrogen in graphite as a function of ion fluence on 60, 100 and 200 keV He^+ ion bombardments.

as the hydrogen concentration decreases. Moreover, the fraction of retained H reaches the constant value of $H/C \approx 0.2$ as the ion fluence increases. The re-emission rates in the beginning of the He^+ ion irradiation increase with decreasing the incident energies. This result corresponds to the energy dependence of the ion-induced re-emission at MeV He^+ ion irradiation, which has already been reported [5,7].

3.2. Analysis of re-emission curves of H

Ion-induced hydrogen release takes place through the following elementary processes: (i) ion-induced detrapping of H from the trapping sites due to displacement collisions with projectile ions or energetic carbon recoils produced by the projectile ions, and (ii) local molecular re-combination of activated (detrapped) hydrogen with trapped one and subsequent fast diffusion of the hydrogen molecule. The activated hydrogen can also be re-trapped into available vacant trapping sites. Thus, the release curve of hydrogen trapped is calculated as the solution of the mass balance equations for free (activated) and trapped hydrogen atoms involving the above elemental processes. When the quasi-equilibrium is reached during ion bombardment, the retained fraction of hydrogen is expressed as a function of ion fluence Φ, as follows [3–5]:

$$\frac{C_0}{n_0}\left(1-\frac{1}{n_T(\Phi)}\right)-\left(1-\frac{K}{\Sigma_T}\right)\ln n_T(\Phi)=-2\sigma_d\frac{K}{\Sigma_T}\Phi, \tag{1}$$

where C_0 and n_0 are the trap density and the initial hydrogen concentration, respectively. In the present study; $C_0/n_0 = 1.0$ because of saturation; Σ_T and K represent the coefficients of the trapping (re-trapping) of the activated hydrogen atom into the vacant trapping sites and the local molecular re-combination between the activated hydrogen and the trapped one; $n_T(\Phi)$ is the fraction of hydrogen retained at Φ with respect to n_0; σ_d is the ion-induced detrapping cross-section.

In the previous paper [5], the values of σ_d were determined by the best fitting Eq. (1) to the experimental release curves of H and D at MeV He^+ ion bombardment. The best fitting was achieved by determination of fitting parameter K/Σ_T which makes the slope to be 45° of log–log plots of $(C_0/n_0)/(1-1/n_T(\Phi))-(1-K/\Sigma_T)\ln n_T(\Phi)$ vs Φ obtained by substitution of the experimental values of the retained fraction into $n_T(\Phi)$. The best fitting parameters of K/Σ_T for H and D were determined to be 0.2 and 0.1, respectively, and the whole release curves were shown to be well reproduced by Eq. (1). The log–log plots of $(C_0/n_0)/(1-1/n_T(\Phi))-(1-K/\Sigma_T)\ln n_T(\Phi)$ vs Φ obtained using the experimental data in Fig. 2 and the value of $K/\Sigma_T = 0.2$ in the similar are shown for incident He^+ ion energies of 60, 100 and 200 keV in Fig. 3. It is seen from Fig. 3 that data points at low ion fluences show a clear proportionality to Φ at low ion fluences, while the data points at high ion fluences deviate gradually and approach to 0.5 as the ion fluence increases.

The deviation of data points at high ion fluences from the proportionality means that the release rate of H is effectively reduced and reaches zero as the concentration of H decreases due to the ion bombardment. It is reasonably explained by extra increase in the re-trapping rate due to increase in vacant trapping sites

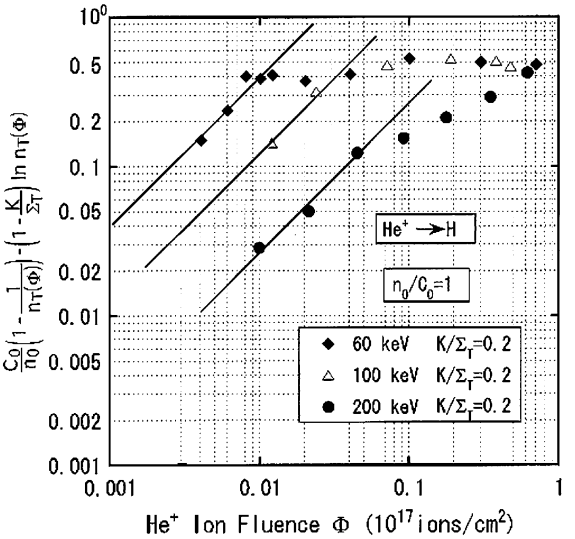

Fig. 3. Log–log plots of $(C_0/n_0)/(1-1/n_T(\Phi))-(1-K/\Sigma_T)\times \ln n_T(\Phi)$ vs He^+ ion fluence Φ calculated from the release curves in Fig. 2. In numerical calculation, the values of K/Σ_T are assumed to be 0.2. The solid lines represent the part of best fitting of Eq. (1) to the experimental one.

concentration surrounding the trapped hydrogen and extra decrease in the local molecular re-combination rate even though the hydrogen is detrapped from the trapping site by the He^+ ion bombardment. If one carbon atom in graphite of the layer structure is able to trap one hydrogen atom, the saturation value of $H/C = 0.4$ means that all the nearest neighbor trapping sites surrounding one trapped hydrogen are vacant. Thus, $H/C \cong 0.2$ suggests that no more than the next nearest neighbor and all the nearest neighbor trapping sites are vacant and they prohibit the trapped hydrogen from the local molecular re-combination with the activated hydrogen due to the geometrical effect in the strong retrapping. The ion-induced detrapping cross-sections σ_d were determined from a part of the proportionality of the data points.

3.3. Discussion of ion-induced detrapping cross-section

The He^+ ion-induced detrapping cross-sections at the incident energies of 60, 100 and 200 keV calculated from the solid lines of Fig. 3 are shown as a function of incident energy in Fig. 4, where the experimental data at the MeV energy [5] are also plotted for comparison. It is seen from Fig. 4 that the cross-sections decrease with increasing incident energy. In the previous paper [4,5], the energy dependence of the He^+ ion-induced detrapping cross-sections was theoretically calculated using Kinchin–Pease model [3] and the Thomas–Fermi potential [8], based on the assumption that ion-induced detrapping of hydrogen takes place due to displacement collisions with energetic carbon recoils produced by He^+ projectile ions in graphite. The values of the cross-section are expressed by the following equation:

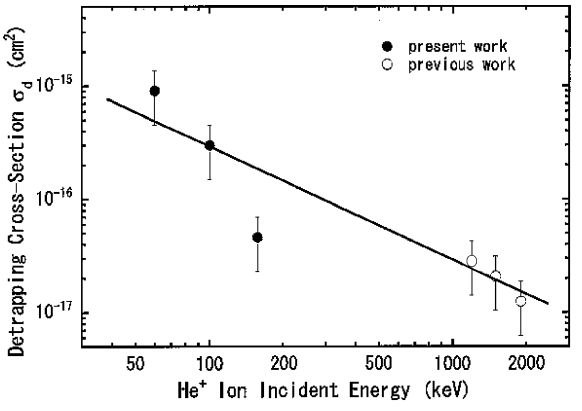

Fig. 4. Energy dependence of the experimental ion-induced detrapping cross-sections. The solid curve represents the theoretical values calculated using the Kinchin–Pease model and the Thomas–Fermi potential.

$$\sigma_d(E_0) = \int_{E_{dC}+E_{dH/v1}}^{E_{P,max}} \frac{\pi}{2}\frac{Z_{He}^2 Z_C^2 e^4}{E_0}\frac{M_{He}}{M_C}\ln\left(\frac{E_{P,max}}{E_{dC}}\right)\frac{dT}{T^2} \times \int_{E_{dC}+E_{dH/v1}}^{T} C_{m_1}^{C\to H}(E_1)^{-m_1}\frac{1}{m_1}\left[\frac{1}{(E_{dH})^{m_1}} - \frac{1}{(v_1E_1)^{m_1}}\right]\frac{1-m}{C_m^{C\to C}}E_1^{-1+2m}dE_1, \quad (2)$$

where T is the energy of the primary knock-on atoms, Z_{He}, Z_C, M_{He} and M_C are the atomic numbers and masses of He and C, respectively; e is the elementary electric charge; E_0, $E_{P,max}$, E_{dC} and E_{dH} are the incident energy, the maximum energy of primary recoiled carbon, the displacement energies for C and H ($E_{dC} = 25$ eV, $E_{dH} = 2$ eV, respectively) [3]. $C_{m_1}^{C-H}$ and C_m^{C-C} are the specific constants of differential cross-sections for C–H and C–C elastic collisions. v_1 is the maximum energy transfer factor in C–H collision, m and m_1 are the power factors for C–C and C–H collisions in the power-law approximation for the Thomas–Fermi potential and are assumed to be $m = 1/3$ and $m_1 = 4/5$ from the energy range in the present study [8].

The theoretical values of He^+ ion-induced detrapping cross-section calculated numerically from Eq. (2) are shown by the solid line in Fig. 4. It is seen from Fig. 4 that the theoretical values show a good agreement with the experimental ones. This indicates that the He^+ ion-induced detrapping of H trapped in graphite takes place due to elastic displacement collisions with energetic carbon recoils above incident energies of 60 keV.

4. Summary

The He^+ ion-induced re-emission of hydrogen implanted in graphite has been measured by means of the H-ERD method with 16 MeV O^{5+} ion beam in the energy range from 60 to 200 keV at room temperature. The concentrations of hydrogen retained in graphite decreased quickly in the beginning of He^+ ion bombardment and attained a constant value equal to half the saturation concentration ($H/C \cong 0.2$). The re-emission curves of H were analyzed using mass balance equations for activated and trapped hydrogen atoms where the elementary processes such as the ion-induced detrapping, the trapping and the molecular re-combination between the activated hydrogen atom and the trapped one were taken into account. The experimental energy dependence of the ion-induced detrapping cross-section obtained was found to be in agreement with the theoretical one calculated using the Kinchin–Pease model and the Thomas–Fermi potential. The detrapping of hydrogen is concluded to take place due to the elastic displacement collisions with energetic carbon recoils produced by He^+ ion bombardment.

References

[1] B. Tsuchiya, K. Morita, J. Nucl. Mater. 226 (1995) 293.
[2] B. Tsuchiya, K. Morita, J. Nucl. Mater. 227 (1996) 195.
[3] K. Morita, Y. Hasebe, J. Nucl. Mater. 176&177 (1990) 213.
[4] Y. Hasebe, M. Sonobe, K. Morita, J. Nucl. Sci. Technol. 29 (1992) 859.
[5] B. Tsuchiya, K. Morita, J. Nucl. Sci. Technol. 31 (1994) 1301.
[6] H.H. Andersen, J.F. Ziegler, Hydrogen Stopping Powers and Ranges in All Element, Plenum, New York, 1977.
[7] J. Roth, B.M.U. Scherzer, R.S. Blewer, D.K. Brice, S.T. Picraux, W.R. Wampler, J. Nucl. Mater. 93&94 (1980) 601.
[8] K.B. Winterbon, P. Sigmund, J.B. Sanders, K. Dan Vidensk, Selsk. Mat. Fys. Medd. 37 (14) (1970).